Beta tACS over rIFG and preSMA Improves Stopping Ability for Younger but not Older Adults

Jane Tan[1], Kartik K. Iyer[2], Michael A. Nitsche[3,4], Rohan Puri[5], Mark R. Hinder[5], Hakuei Fujiyama[1,6,7]

[1]Discipline of Psychology, College of Science, Health, Engineering and Education, Murdoch University, Perth, Australia

[2]QIMR Berghofer Medical Research Institute, Brisbane, Australia

[3]Leibniz Research Centre for Working Environment and Human Factors, Department of Psychology and Neurosciences, Dortmund, Germany

[4] Bielefeld University, University Hospital OWL, Protestant Hospital of Bethel Foundation, University Clinic of Psychiatry and Psychotherapy and University Clinic of Child and Adolescent Psychiatry and Psychotherapy, Germany

[5]Sensorimotor Neuroscience and Ageing Research Group, School of Psychological Sciences, College of Health and Medicine, University of Tasmania, Hobart, Australia

[6] Centre for Healthy Ageing, Health Futures Institute, Murdoch University, Western Australia, Australia

[7] Centre for Molecular Medicine and Innovative Therapeutics, Murdoch University, Western Australia, Australia.

Corresponding Author:
Jane Tan
Discipline of Psychology, College of Science, Health, Engineering and Education, Murdoch University, Perth, Australia
90 South Street, Murdoch, WA, 6500, Australia
e-mail: j.hl.tan@gmail.com

Abstract

A growing body of research suggests that changes in both structural and functional connectivity in the aging brain contribute to cognitive declines observed in later life. In recent years, transcranial alternating current stimulation (tACS) has garnered substantial research interest as a potential tool for the modulation of functional connectivity. Here, we report the findings from a double-blind crossover study that investigated the effects of dual-site beta tACS over the right inferior frontal gyrus (rIFG) and pre-supplementary motor area (preSMA) on the response inhibition performance of healthy older (n =15, aged 61-79 years) and healthy younger (n = 18, aged 18-34 years) adults. Two tACS conditions were administered in separate sessions: in-phase tACS, where electrical currents delivered to rIFG and preSMA have a 0° phase difference, and anti-phase tACS, where the currents have a 180° phase difference. In-phase tACS was found to significantly improve response inhibition of only younger individuals, with better inhibitory performance associated with stronger rIFG-preSMA functional connectivity. Despite no significant changes in response inhibition performance of the older adults, their task-related EEG data suggest potential increases in proactive inhibition resulting from in-phase tACS. Anti-phase tACS did not result in any significant changes in response inhibition or functional connectivity for either age group. The current study sheds light on the complex nature of responses to non-invasive brain stimulation, which potentially contributes to the development of novel neuromodulation-based therapeutic interventions for the maintenance of cognitive function in older adults.

Keywords: *age-related decline; response inhibition; stop-signal task; transcranial alternating current stimulation; inferior frontal gyrus; pre-supplementary motor area*

1. Introduction

Response inhibition, or the ability to suppress or cancel a pre-potent motor action, is a fundamental cognitive function that is crucial for flexible adaption to a changing external environment (Miyake et al., 2000). However, response inhibition tends to decline as we age (e.g., Hermans et al., 2018), with deleterious effects on the ability of older adults to engage in daily activities safely and independently. Indeed, poorer response inhibition has been linked to a higher risk of falls for older individuals (Schoene et al., 2017). The development of effective and reliable interventions to alleviate age-related inhibitory deficits could therefore play a critical role in improving the well-being of elderly populations.

There is mounting evidence suggesting that age-related changes in the structural and functional connections within brain networks contribute to age-related cognitive declines. Greater declines in executive functioning and attention have been associated with lower white matter structural integrity and decreased segregation of brain networks such as the default mode network and executive control network (Brown et al., 2019; Chong et al., 2019). Notably, the functional connectivity between the right inferior frontal gyrus (rIFG), pre-supplementary motor area (preSMA), and sensorimotor regions was found to play a progressively larger role in response inhibition performance as individuals get older (Tsvetanov et al., 2018). It has been postulated that functional interactions between the rIFG and preSMA subserve connectivity within the fronto-basal-ganglia network, which underlies response inhibition performance (Xu et al., 2016). As outlined in a previous review (Tan et al., 2019), facilitating the functional connectivity between the rIFG and the preSMA, by way of non-invasive brain stimulation, may aid in the mitigation of age-related inhibitory deficits.

In recent years, transcranial alternating current stimulation (tACS) – a form of non-invasive brain stimulation – has garnered substantial research interest as a potential tool for

the modulation of functional connectivity. This technique involves the application of weak alternating electrical currents through electrodes placed over the scalp and has been primarily used to modulate neural oscillatory activity (Antal & Herrmann, 2016). While in-depth understanding of tACS mechanisms is still being advanced by emerging research, there is evidence to support the frequency-specific entrainment of neural activity during tACS application. For instance, the phase-locking of endogenous neural activity to the stimulation frequency was found to be significantly stronger during real tACS when compared with sham stimulation (Helfrich, Schneider, et al., 2014; Wischnewski et al., 2018). Single-neuron recordings in non-human primates during tACS administration indicated that spike timings occured preferentially around the 0º phase of each tACS cycle, and exhibited higher phase-locking values when compared with sham stimulation (Krause et al., 2019).

Based on the same philosophy of entrainment, tACS has been shown to exert modulatory effects on the oscillatory phasic relationships *between* distinct cortical regions. Through the simultaneous recording of electroencephalographic (EEG) activity during tACS application, the delivery of alternating currents at the same phase (in-phase, i.e., with 0º phase difference) to two brain regions (i.e., dual-site) was shown to strengthen the frequency-specific phase-coupling of electrophysiological signals between those stimulated sites (Helfrich, Knepper, et al., 2014; Schwab et al., 2019). The effects of dual-site tACS have also been found to be phase-dependent, such that the phase-synchronisation of two regions was weakened when tACS currents were delivered at a 180º phase difference (i.e., anti-phase tACS) (Helfrich, Knepper, et al., 2014). The increase in phase-coupling elicited by in-phase tACS was also significantly larger when compared with that of jittered-phase and sham stimulation (Helfrich, Knepper, et al., 2014; Schwab et al., 2019). These findings support the communication-through-coherence theory, which posits that the strength of inter- and intra-regional connectivity in the brain is underpinned by the oscillatory phase relationships of

neuronal groups, with higher phase coherence facilitating neuronal information transfer and functional connectivity (Fries, 2005, 2015; Womelsdorf et al., 2007). Furthermore, phase-coherent neural oscillations are thought to be spectral signatures of the large-scale/inter-regional interactions between and within neural networks that underlie cognitive processing (Salinas & Sejnowski, 2001; Siegel et al., 2012). Crucially, Polanía et al. (2012) found evidence suggesting that inter-regional phase-coupling is *causally* involved in cognitive functioning. Through the application of dual-site theta tACS to left fronto-parietal sites, the authors observed in-phase tACS resulted in significantly improved verbal working memory when compared with sham and anti-phase stimulation (Polanía et al., 2012). Similarly, the delivery of in-phase gamma tACS to interhemispheric parietal-occipital regions was shown to improve motion perception performance relative to anti-phase stimulation, a likely consequence of the stronger functional coupling between the stimulated regions that resulted from in-phase tACS (Helfrich, Knepper, et al., 2014).

In light of the mounting evidence of strong associations between age-associated changes in functional networks and cognitive functioning, it was postulated that the facilitatory effects of in-phase tACS on functional connectivity can be harnessed for the alleviation of age-related cognitive declines (Tan et al., 2019). Indeed, this hypothesis was corroborated by Reinhart and Nguyen's (2019) study, which found that in-phase tACS over fronto-temporal regions significantly improved the working memory performance of older adults, with stronger theta phase-coupling between the stimulated regions. To our knowledge, their findings constitute the first empirical evidence that this conceptual framework can be applied to the aging brain for the improvement of cognitive functions. The main objective of the current study was to examine the viability of this approach within the context of response inhibition. Namely, to determine if a dual-site tACS protocol that is designed to facilitate

neural oscillatory phase-coupling can strengthen the functional connectivity between rIFG and preSMA and improve response inhibition in healthy older adults (Tan et al., 2019).

Using a double-blind crossover design, the current study investigated the effects of dual-site beta tACS over the rIFG and preSMA in older and younger adults on response inhibition; changes in functional connectivity before and after stimulation were assessed using a series of EEG measures. Beta (20 Hz) was chosen as the stimulation frequency in view of its putative role in information transfer within the fronto-basal-ganglia network during response inhibition (Aron et al., 2016; Swann et al., 2011). Our primary hypothesis was that dual-site tACS would modulate response inhibition and resting-state functional connectivity in a phase-dependent and frequency-specific manner: in-phase stimulation was expected to facilitate beta-band phase-coupling between the stimulated regions and improve response inhibition of participants in both age groups. Conversely, anti-phase tACS was anticipated to hinder response inhibition and weaken the phase connectivity between the rIFG and preSMA.

2. Materials and Methods

2.1. Design

A crossover design was used, where participants from two age groups (older and younger) underwent two stimulation conditions (in- and anti-phase tACS) that were administered in separate sessions (Figure 1). The sessions (counterbalanced between participants) were spaced at least a week apart and conducted at the same time of day. Resting-state (eyes-open and eye-closed; 3 min each) and task-related EEG activity were recorded before and after the administration of tACS. However, only eyes-opened activity was analysed as some participants reported having fallen asleep during the recording of eyes-closed activity. Furthermore, analysis of eyes-opened resting-state activity is recommended

for experimental designs utilising tasks that require visual processing (Barry et al., 2007), such as the stop-signal task in the current study. Task-related activity was measured during the performance of the stop-signal task (described below).

Figure 1

Experimental Protocol

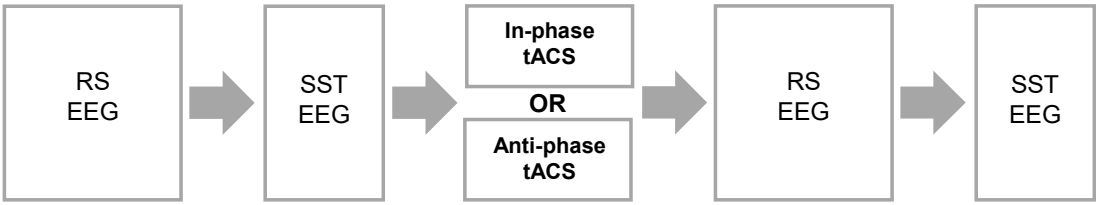

Note. Resting-state (RS) and task-related EEG activity were measured before and after tACS. Task-related activity was recorded during stop-signal task (SST) performance. The two tACS conditions, in- and anti-phase, were administered in separate sessions for all participants.

2.2. Participants

Power analysis (power = 0.80; α = .05) indicated that 12 participants for each age group were required for an expected medium effect size of improved response inhibition by in-phase tACS. This effect size was based on the findings of previous studies that had investigated the effects of transcranial electrical stimulation on response inhibition (e.g., Hogeveen et al., 2016). In consideration of possible attrition, excessively noisy EEG recordings, and task performance where the failed stop probability was < 0.25 or > 0.75 (see Section 2.6.1; Verbruggen et al., 2019), a total of 41 participants (20 younger and 18 older adults) were recruited. The data of 5 participants were excluded from all analyses: two (1 younger, 1 older) were excluded due to excessive movement artifacts in their EEG recordings, and three (1 younger, 2 older) were excluded because of their stop-signal task performance (see Results section 3.2.1.). The final dataset thus comprised 33 participants,

with 18 younger participants (11 females; mean age = 23.56 years, *SD* = 4.49 years) and 15 older participants (10 females; mean age = 68.80 years, *SD* = 5.39 years).

All participants were right-handed according to the Edinburgh Handedness Inventory (Oldfield, 1971; older participants: Laterality Quotient, LQ = 84.67 ± 18.85; younger participants: LQ = 83.33 ± 15.34). The Montreal Cognitive Assessment (MoCA; Nasreddine et al., 2012) was used to screen older participants for possible cognitive deficits, and all of them met the recommended cut-off score of 23 suggesting no deficits (Carson et al., 2018; 28.33 ± 1.40). None of the participants reported any existing neurological conditions, metal implants or implanted neurostimulators, cochlear implants, cardiac pacemaker, and intra-cardiac lines. Apart from one older individual who was on a non-steroidal aromatase inhibitor, none of the participants were on psychoactive medications.

To assess possible confounds to behavior and neurophysiology, participants were asked during each session to report their quality of sleep and number of hours slept during the previous night, and the amount of caffeine and alcohol they had consumed within 12 hours prior to the experimental session. A questionnaire was also administered to assess the occurrence and intensity of sensations (e.g., itching and tingling) that participants might have experienced while receiving tACS (Fertonani et al., 2015).

This study was approved by the Murdoch University Human Research Ethics Committee (2016/021). Participants provided written informed consent before taking part in the experiment and were remunerated with either academic credits or cash payments of $20 per session.

2.3. Stop-Signal Task

Response inhibition performance was assessed using a stop-signal task, whereby inhibitory performance was operationalized with the stop-signal reaction time (SSRT). The

SSRT measures the amount of time needed to cancel an ongoing motor response upon the onset of a stop signal (Logan & Cowan, 1984). The task was programmed with PsychoPy (version 1.83.04; Peirce et al., 2019) and displayed on a computer monitor with a refresh rate of 144 Hz.

Each trial began with a primary task, where a fixation cross was presented for a time interval that was jittered between 250 and 750 ms before the onset of an imperative signal, which was a green circle. Participants were asked to respond as quickly as possible by pressing the space bar on a computer keyboard with their right index finger whenever the imperative signal was presented (Figure 2).

Figure 2

The Stop-Signal Task

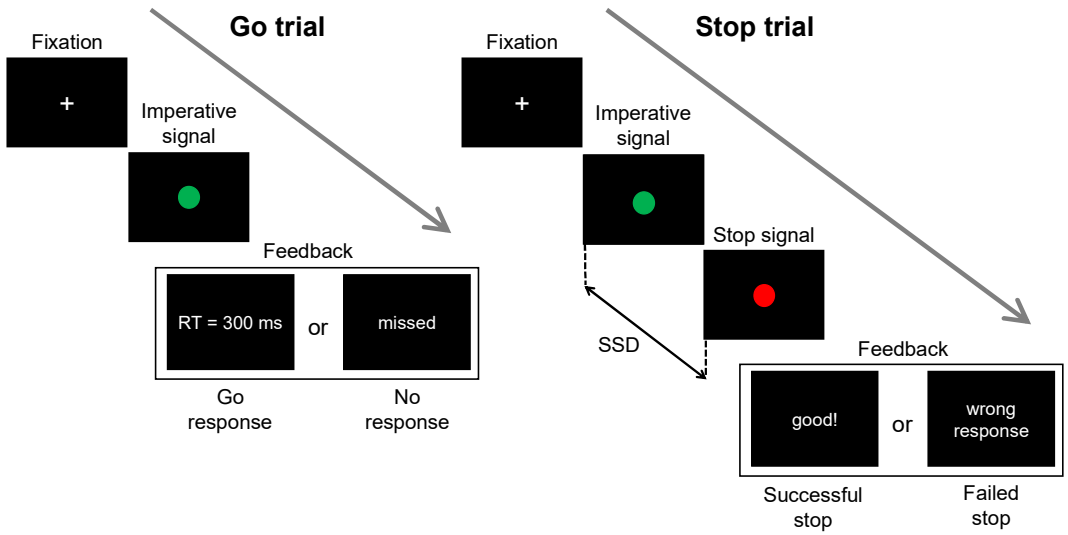

Note. The imperative signal was a green circle, to which participants were asked to respond as quickly as they could by pressing the space bar on a computer keyboard. During stop trials, the imperative signal was followed after a stop-signal delay (SSD) by the stop signal, which was a red circle. Participants had to refrain from responding, i.e., cancel and inhibit their response to the imperative signal, upon presentation of the stop signal.

The majority of trials (70% of total trials) were ‘go’ trials, whereby the imperative signal was presented for a maximum of 1500 ms, or until a response was provided. This was followed by the display of feedback for 1000 ms, where the participant’s reaction time (the

duration from imperative signal onset to response) was displayed. If no response was provided within the 1500-ms time limit, 'missed' was displayed on the screen.

During stop trials (30% of total trials; randomly interspersed in each block), the imperative signal was replaced by the stop signal, which was a red circle, after a stop-signal delay (SSD). The initial SSD was set at 50 ms. During stop trials, participants had to attempt to cancel (inhibit) the go response and *not* press the space bar. Stop signals were displayed for 1000 ms, or until a response (a failed stop) occurred. The trial feedback – 'good!' for successful stops and 'wrong response' for failed stops – was then displayed for 1000 ms.

The SSD was adjusted in a staircase fashion, wherein a successful stop would result in an increase in SSD of 50 ms for the following stop trial, while a failed stop would result in SSD being reduced by 50 ms for the subsequent stop trial. The minimum SSD was 50 ms. This tracking procedure is intended to result in the probability of a failed stop, P(Respond|Stop), being ~ 0.5, thus improving the reliability of SSRT estimates (Band et al., 2003; Verbruggen et al. 2019).

Participants performed a practice block of 20 trials (6 stop trials) before the first pre-tACS behavioral assessment to ensure that they understood and adhered to task instructions (Verbruggen et al., 2019). The practice block was administered a second time for individuals who might not have understood or adhered to the task instructions during the first practice block (e.g., if a participant appeared to have delayed their response to the imperative signal in anticipation of the stop signal). Two blocks of the stop-signal task were administered at each assessment time (pre-tACS and post-tACS). Each assessment block contained 100 trials (block duration: ~4 min; 30 stop trials per block).

2.4. tACS

High-definition tACS was delivered double-blind, using a neuroConn DC-Stimulator MC (neuroCare Group GmbH). Rubber disc electrodes of 2 cm diameter were placed on the scalp using Ten20 conductive paste in a 2 X 1 montage for each stimulation site (see Figure 3). The rIFG was localized at the intersection point of the line between T4 and Fz, and the line between F8 and Cz (10-10 electrode positions; Chatrian et al., 1985; Jacobson et al., 2011). The preSMA was localized at Fz (Hsu et al., 2011). Electrode impedance was kept below 50 kΩ. Sinusoidal currents at 20 Hz (beta frequency) with zero DC offset were applied for a stimulation duration of 20 minutes, with a 30 s ramp-up/down of currents at the beginning and end of stimulation.

The electric field model is depicted in Figure 3. The currents were applied with peak-to-peak amplitudes of 1 mA to both stimulation sites at 0º phase lag and 180º phase lag for in-phase and anti-phase tACS conditions, respectively.

Figure 3

Current Flow Model

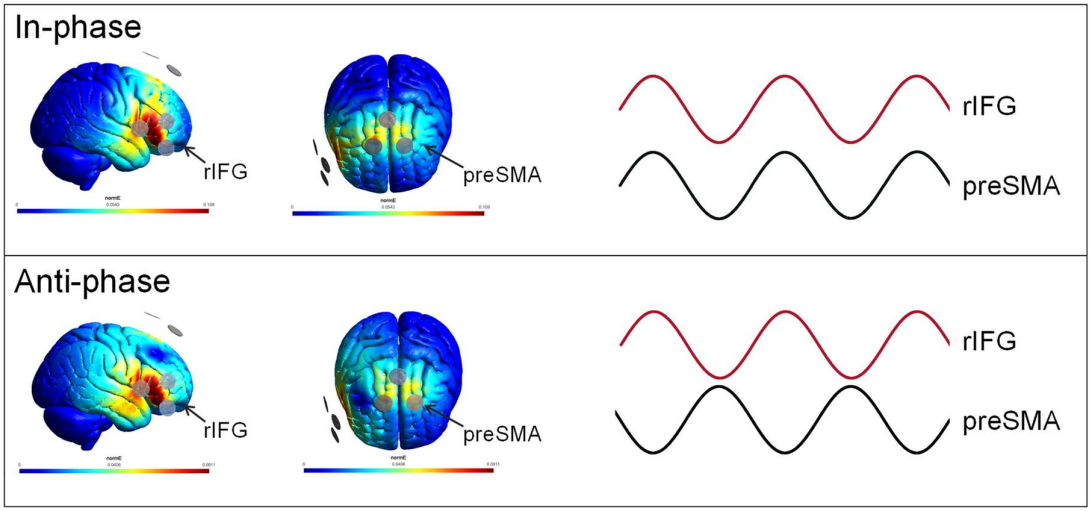

Note. A 2 X 1 electrode montage was used for each stimulation site. Currents with peak-to-peak amplitudes of 1 mA were delivered to the stimulation sites with a 0° and 180° phase difference for in-and anti-phase tACS, respectively.

2.5. EEG Acquisition and Preprocessing

EEG was recorded using a Net Amps 300 amplifier and Net Station (4.5.6) software, with 128-channel HydroCel Geodesic Sensor Nets (GSN, Magstim EGI; egi.com) and the GSN 128 1.0 montage. Data were acquired at a sampling rate of 1000 Hz, and online referenced to the vertex (Cz). Impedance was kept below 50 kΩ. The EEG signals were high-pass filtered at 0.1 Hz and low-pass filtered at 500 Hz during recording.

The EEG data were preprocessed with the EEGLAB toolbox (Delorme & Makeig, 2004) through the MATLAB environment (MathWorks, R2020a). The data were down-sampled to 500 Hz, bandpass filtered from 1 to 85 Hz, and notch filtered at 50 Hz. Resting-state data were divided into 2 s epochs. Task-related data were epoched into time windows that were time-locked to the stop signal (-500 to 1200 ms) and baseline-corrected using prestimulus activity from -500 to 0 ms. The epoched data were visually inspected, with bad channels and noisy epochs manually removed. Following the interpolation of removed channels, the *fullRankAveRef* EEGLAB plugin was used to re-reference the data to the average. Finally, an independent component analysis (Informax algorithm) was conducted and the components were visually inspected for the visual detection and removal of ocular, vascular, and myogenic artifacts.

A surface Laplacian spatial filter was applied to both task-related and resting-state data. This filter improves the spatial resolution of scalp-level activity by attenuating spatially-broad activity that is likely due to volume conduction (Nunez & Srinivasan, 2006). The surface Laplacian was computed using Perrin et al.'s (1989) spherical spline method (smoothing parameter of 10-5 and Legendre polynomial order of 40) with the MATLAB implementation by Cohen (2014).

2.6. Data Analyses

2.6.1. Stop-Signal Task Performance

SSRTs were estimated with the integration method, which involves the subtraction of the mean SSD from the nth reaction time at which the integral of the go RT (reaction time of go trials) distribution equals zero (Logan & Cowan, 1984). While the integration method does not require that P(Respond|Stop) = 0.5, probabilities that are close to 0.5 were found to improve the reliability of SSRT estimates (Band et al., 2003). For that reason, the data from participants with P(Respond|Stop) that were lower than 0.25 or higher than 0.75 were excluded from all analyses (Congdon et al., 2012; Verbruggen et al., 2019). We assessed this via stop accuracy, the inverse construct of P(Respond|Stop), i.e., the proportion of correctly inhibited trials.

Shapiro-Wilk statistics and the visual inspection of histograms and QQ-plots revealed that the data for SSRTs and go RTs were not normally distributed. Consequently, planned comparisons using Wilcoxon signed-rank tests were performed to assess the pre-post changes in these outcome variables for each tACS condition and age group. Effect sizes were measured with the Wilcoxon effect size, r, which was calculated with the R package rstatix's *wilcox_effsize* function as the z statistic divided by square root of the sample size ($z/\sqrt{n}$), with $r \leqslant 0.1$ for small effects, $0.1 < r \leqslant 0.5$ for medium effects, and $r > 0.5$ for large effects (Kassambara, 2021).

2.6.2. Imaginary Component of Coherency (ImCoh)

The analyses of rIFG-preSMA connectivity were performed on signals that were recorded from the following EEG channel sensors: F4 and F6 for rIFG, and Fz and AFz for preSMA. As with the placement of the tACS electrodes, the selection of the EEG channels

that corresponded to the rIFG and preSMA was based on the 10-10 electrode positions of previous transcranial electrical stimulation studies (Hsu et al., 2011; Jacobson et al., 2011).

The preprocessed EEG time series data were convolved with complex Morlet wavelets in 1-Hz increments for frequencies between 8 and 45 Hz. The wavelet lengths ranged from 4 to 10 cycles in 38 linearly-spaced steps, with the wavelet length increasing with the wavelet frequency for the dynamic adjustment of the balance between temporal and frequency precision (Cohen, 2014). To minimize the effects of edge artifacts, the resultant analytic signals were analysed in time windows of 400 to 1600 ms in each epoch for resting state data and -200 to 800 ms for task-related data.

The imaginary component of coherency (ImCoh), an index of the consistency of phase angle differences (phase lag) between signals (Nolte et al., 2004), was used to assess changes in phase-coupling that were induced by tACS. For channels *i* and *j*, with the complex Fourier transforms $x_i(f)$ and $x_j(f)$ of their time series data, ImCoh at frequency *f* is given as

$$\left| Imaginary\left(\frac{S_{ij}(f)}{\sqrt{S_{ii}(f)S_{jj}(f)}}\right)\right|$$

where the cross-spectral density $S_{ij}(f)$ is derived from the complex conjugation of $x_i(f)$ and $x_j(f)$. The coherency between the channel signals is obtained by normalising the cross-spectral density by the square root of the signals' spectral power ($S_{ii}(f)$and $S_{jj}(f)$). The result is a complex number from which the imaginary component, ImCoh, is extracted. ImCoh has been shown to be insensitive to the effects of volume conduction, and its usage thus reduces the likelihood of mistakenly taking spurious connectivity for real functional coupling (Nolte et al., 2004). An ImCoh value of 1 denotes perfect phase-coupling between signals, while a value of zero indicates that the phase angle differences between the signals are completely random. The ImCoh was calculated for each inter-site channel-pair (F4-Fz,

F6-Fz, F4-AFz, and F6-AFz) and subsequently averaged across the channel-pairs to result in the mean ImCoh estimate between the rIFG and preSMA (rIFG-preSMA ImCoh for brevity).

The estimates of ImCoh were computed at the trial-level, in sliding time windows with frequency-varying lengths of 3-8 cycles in 38 linearly-spaced steps, at 20-ms intervals within each epoch. For resting-state data, these estimates were subsequently averaged within and across epochs to obtain an ImCoh estimate for every participant at pre- and post-tACS for in- and anti-phase tACS sessions. The ImCoh estimates for task-related data were baseline-corrected to -200-0 ms from stop-signal onset and averaged across epochs at each time point. This was conducted for the stop trials of every participant at pre- and post-tACS for in- and anti-phase tACS sessions.

To determine the frequency-specificity of tACS-induced effects on ImCoh, we assessed the changes in rIFG-preSMA ImCoh from pre- to post-tACS for each age group and tACS condition. This was performed with ImCoh estimates from resting-state data and from successful stop trials for task-related data. Through cluster-based permutation testing, the ImCoh values at pre- and post-tACS were contrasted at each sample, i.e., frequency point for resting-state data and time-frequency point for task-related data. This non-parametric statistical approach allows multiple univariate tests to be carried out for each sample while controlling for the family-wise error rate (Maris, 2012; Maris et al., 2007). The permutation distributions of maximum cluster sizes were constructed with 2000 permutations. In each permutation, the session time labels (i.e., pre-tACS and post-tACS) were randomly assigned to the ImCoh values at each sample. A paired-sample *t*-test was performed to compare the ImCoh values between the randomly assigned time labels at each sample.

The correlation between rIFG-preSMA ImCoh and response inhibition performance was also analysed with cluster-based statistics. For each age group at each session time and

tACS condition, the SSRTs and sample-level ImCoh values were ranked across participants. The ranking values were subsequently used for the computation of the Spearman's correlation coefficient (ρ) between SSRTs and sample-level ImCoh values. For the thresholding of sample points, ρ values were converted into t values using the formula:

$$t = \frac{\rho * sqrt(N-2)}{sqrt(1-\rho^2)}$$

where N was the number of participants in the subgroup that was being analysed. In every permutation, the SSRT ranking values were randomly shuffled at every sample point across participants before the computation of ρ.

The same cluster-based approach was used to analyse the correlation between the change from pre- to post-tACS for ImCoh ($\Delta ImCoh = ImCoh_{post\text{-}tACS} - ImCoh_{pre\text{-}tACS}$) and response inhibition performance ($\Delta SSRT = SSRT_{post\text{-}tACS} - SSRT_{pre\text{-}tACS}$). The ΔSSRT and ΔImCoh at each sample point were ranked across participants and the correlation between their ranking values was assessed with Spearman's ρ. During each permutation, the ranking values for ΔSSRT were randomly shuffled at each sample across participants before ρ was computed. The ρ value for each sample point was converted into a t value for thresholding.

The cluster-based permutation tests were performed with $\alpha = .05$ for the thresholding of statistical test values (e.g., t values) at each sample point. Sample points with suprathreshold values were clustered according to spectral adjacency for resting-state data, and temporal and spectral adjacency for task-related data, with separate clusters for positive and negative values. The size of each cluster was obtained by taking the sum of the absolute statistical values within the cluster. The permutation distribution was constructed with the largest cluster size of every permutation, and its 97.5th percentile was set as the cluster-level correction threshold. The clusters in the real (i.e., not permuted) data with cluster sizes that exceeded this threshold were deemed to be significant.

Unless otherwise stated, statistical analyses and visual illustration of the results were performed via customized scripts in MATLAB (MathWorks, R2020a), and the software package R for Statistical Computing version 3.6 (R Core Team, 2019) using packages 'tidyverse' (Wickham, 2021), 'ggpubr' (Kassambara, 2020), 'DescTools' (Signorell, 2021), 'janitor' (Firke, 2021), 'reshape2' (Wickham, 2020), 'rcompanion' (Mangiafico, 2021), 'car' (Fox et al., 2020), 'heplots'(Fox & Friendly, 2021) , 'rstatix' (Kassambara, 2021), 'Hmisc' (Harrell, 2021), 'RColorBrewer' (Neuwirth, 2014), and 'hrbrthemes' (Rudis, 2020).

2.6.3. Data and Code Availability

Data are available upon request to the authors, subject to approval from Murdoch University Human Research Ethics Committee. Analysis codes are publicly available on the Open Science Framework (OSF): https://osf.io/te9zn/.

3. Results

Unless otherwise stated, data are expressed as mean (*M*) ± standard deviation (*SD*), and significance was based on an alpha level of 0.05.

3.1. Control Measures

There were no significant differences in perceived tACS sensations, sleep quality, sleep quantity, caffeine intake, and alcohol intake between the different tACS conditions (see Supplementary Material, Tables S1-S2). This suggests that our findings were unlikely to have been significantly impacted by these potential confounds and that the participants were effectively blinded to the stimulation conditions.

3.2. Stop-Signal Task Performance

The descriptive statistics of SSRTs and go RTs are summarized in Table 1.

Table 1

Stop-Signal Task Performance

	Older				Younger			
	In-Phase tACS		Anti-Phase tACS		In-Phase tACS		Anti-Phase tACS	
Outcome variable	Pre	Post	Pre	Post	Pre	Post	Pre	Post
SSRT (ms)	223.76 ± 33.78	217.55 ± 33.10	231.06 ± 29.35	223.38 ± 29.94	188.84 ± 31.41	176.79 ± 32.13	183.71 ± 28.48	174.88 ± 39.36
Go RT (ms)	481.29 ± 90.22	529.31 ± 84.29	489.12 ± 72.82	521.86 ± 104.49	302.34 ± 57.21	289.37 ± 49.40	304.96 ± 56.35	301.62 ± 56.77

Note. Data are expressed as mean ± standard deviation.

Following in-phase tACS, SSRTs (Figure 4A) were significantly shorter at post-tACS compared to pre-tACS in the younger participants, $Z = 131$, $p = 0.048$, $r = 0.467$ (medium effect size), suggesting that in-phase tACS improved response inhibition in young adults. Conversely, for the older individuals, while a similar pattern was present, the reduction in their SSRTs from pre- to post-tACS was not statistically significant, $Z = 72$, $p = 0.524$, $r = 0.176$ (small effect size). Anti-phase tACS did not result in any significant differences between pre-tACS and post-tACS SSRTs for both younger and older participants (Zs ≤ 115.00, ps ≥ 0.212).

The go RTs (Figure 4B) of the younger group were significantly shorter at post-tACS after in-phase stimulation, compared to pre-tACS: $Z = 149$, $p = 0.004$, $r = 0.652$ (large effect size). A reversed pattern was observed for older participants after receiving in-phase stimulation, with significantly longer go RTs at post-tACS relative to pre-tACS, $Z = 14$, $p = 0.007$, $r = 0.675$ (large effect size). Unlike in-phase tACS, anti-phase tACS did not result in significant changes in go RTs from pre- to post-stimulation for both younger and older participants (Zs ≤ 101.00, ps ≥ 0.095).

The descriptive statistics of failed stop RTs (reaction times on failed stop trials), stop accuracy, and go accuracy, and their changes from pre- to post-tACS are included in the Supplementary Material.

Figure 4

Stop-Signal Task Performance

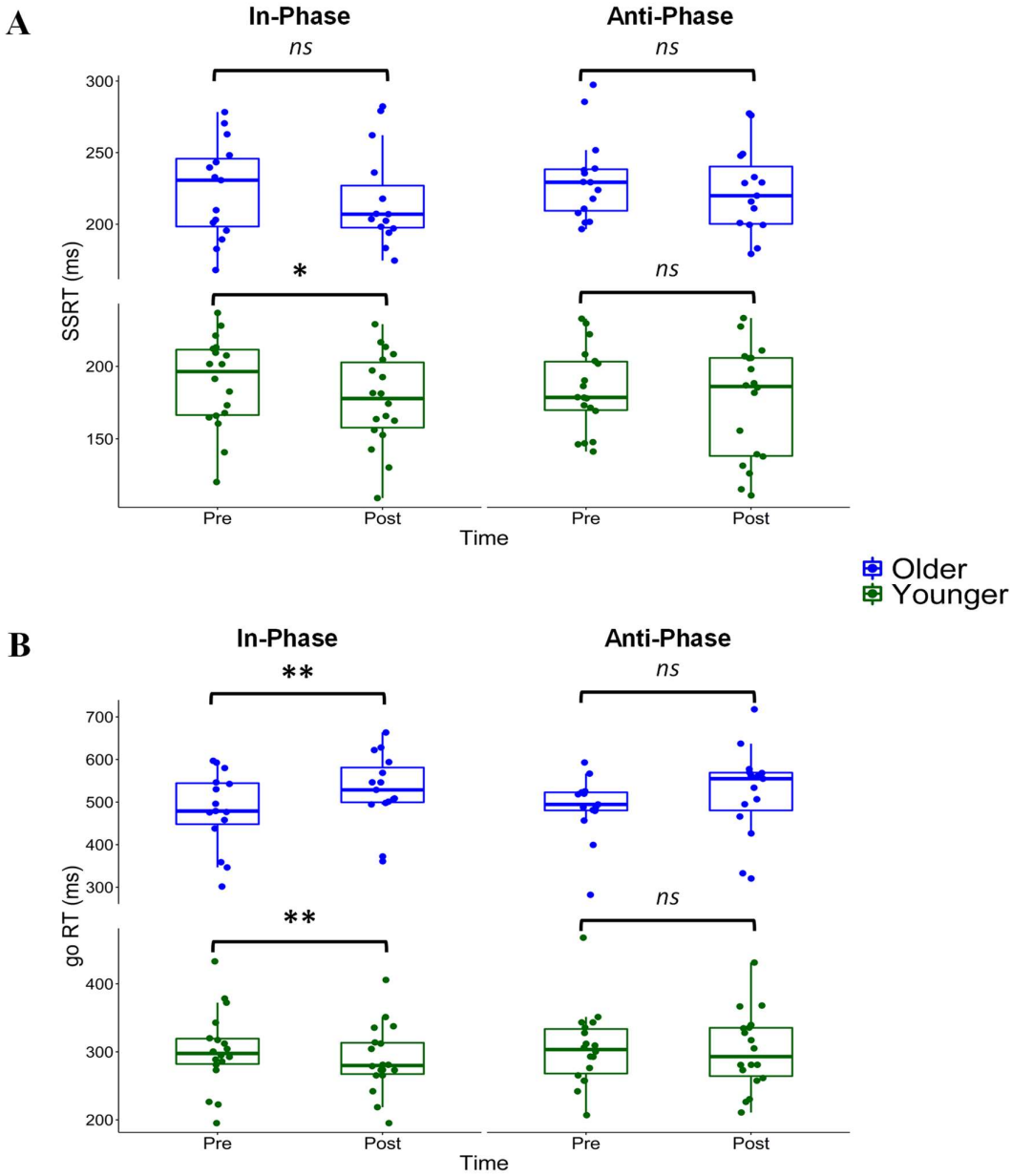

Note. **A**. The SSRTs of younger participants were significantly shorter after in-phase tACS. **B**. The go RTs of younger participants were significantly shorter after in-phase tACS, while the go RTs of the older participants were significantly longer after in-phase tACS. *ns*: not significant.
* $p < 0.05$, ** $p < 0.01$.

3.3 Resting-State ImCoh

3.3.1. In-Phase tACS Significantly Modulated the Brain-Behavior Relationship Between SSRTs and Resting-State ImCoh

Cluster-based permutation testing found no significant differences between the pre- and post-tACS estimates of resting-state ImCoh for in-phase or anti-phase tACS in younger and older participants (see Supplementary Figures S1 and S2).

Resting-state ImCoh was not significantly associated with SSRTs at pre-tACS for both younger and older participants in both in-phase and anti-phase sessions (Supplementary Figure S3). However, resting-state ImCoh (17-41 Hz) was significantly and negatively associated with SSRTs for the younger participants after in-phase tACS, indicating that greater functional connectivity after in-phase tACS was associated with shorter SSRTs (i.e., faster response inhibition) (Figure 5). Notably, this change in brain-behavior relationship occurred in conjunction with the younger participants' significant improvement in SSRTs after in-phase tACS. By contrast, the SSRTs and resting-state ImCoh of younger participants were not significantly correlated after they received anti-phase tACS (Supplementary Figure S3). For older participants, there were no significant correlations between their SSRTs and resting-state ImCoh during pre- and post-tACS for both in-phase and anti-phase tACS sessions (Supplementary Figure S3). There were no significant correlations between ΔImCoh and ΔSSRT after in- and anti-phase tACS for both older and younger participants (Supplementary Figure S4).

Figure 5

Cluster-Based Analyses of Correlation Between Resting-State ImCoh and SSRTs Before and After In-Phase tACS for Younger Participants

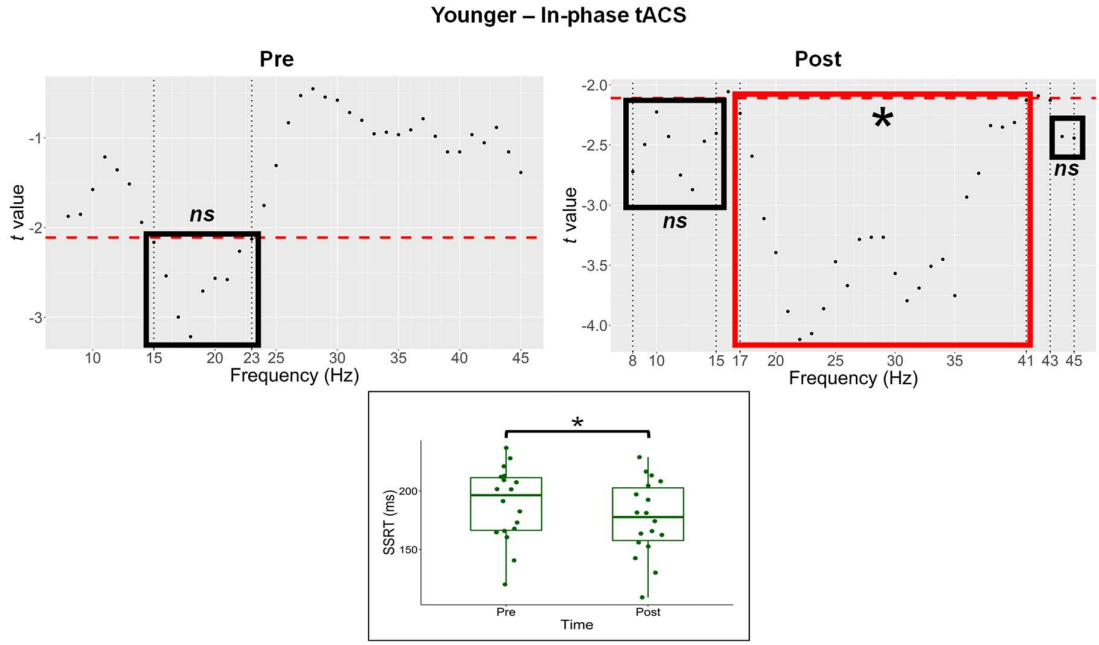

Note. **Top**. The *t* values (converted from Spearman's ρ) for the correlation between SSRTs and ImCoh at each spectral point. The red dashed lines represent the uncorrected threshold, i.e., critical *t* at α = .05 before cluster-based correction. Clusters of contiguous samples with suprathreshold *t* values are encased in boxes. There was a significant cluster of negative *t* values spanning 17-41 Hz (red box) for the younger participants after receiving in-phase tACS, indicating that higher ImCoh values were associated with shorter SSRTs. The remaining clusters (black boxes) were not significant after cluster-based correction. *ns*: not significant after cluster-based correction. *significant after cluster-based correction set at 97.5th percentile of permutation distribution. **Bottom (from Figure 4A)**. The change in brain-behavior relationship occurred in conjunction with the younger participants' significant decrease in SSRTs (better response inhibition) after in-phase tACS. * $p < 0.05$

3.3.2. Ruling Out Potential Confounds

To assess the spatial-specificity of the above findings, we performed the same analyses on the ImCoh values between the preSMA and the control site of the *left* IFG (lIFG; EEG channels at F5 and F3). The findings indicated that there were no significant pre-post changes in lIFG-preSMA ImCoh from in- and anti-phase tACS for both younger and older participants (Supplementary Figure S5). There were also no significant correlations between lIFG-preSMA ImCoh and SSRTs at pre- and post-tACS, and in- and anti-phase stimulation,

for younger and older participants (Supplementary Figure S6). The correlation between ΔImCoh for lIFG-preSMA and ΔSSRTs was also not significant (Supplementary Figure S7). These findings support the spatial specificity of the change in correlation between rIFG-preSMA ImCoh and SSRTs after in-phase tACS for the younger participants (Figure 5).

Changes in EEG coherency (and its imaginary component) between two channels can also be due to changes in their spectral power instead of real changes in phase-coupling (Nolte et al., 2004). To determine if the results of our ImCoh analyses might be confounded by significant changes in oscillatory power, we also examined the effects of tACS on spectral power during resting-state and successful stop trials (see Supplementary Material for details). There were no significant changes in spectral power at the preSMA or rIFG after in- or anti-phase tACS, for both younger and older participants (Supplementary Figure S8). There were also no significant correlations between SSRTs and spectral power at the preSMA and rIFG for any of the tACS conditions, age groups, and session times (Supplementary Material Figures S9 and S10). This suggests that the tACS-induced changes in correlation between resting-state ImCoh and SSRTs (Figure 5) were unlikely caused by changes in spectral power. The correlations between ΔPower and ΔSSRT were also not significant for both tACS conditions and age groups (Supplementary Figure S11).

3.4. Task-Related ImCoh

3.4.1. Inconsistencies in the Brain-Behavior Relationship between SSRTs and Task-Related ImCoh

Cluster-based permutation tests found no significant differences in the pre- and post-tACS estimates of ImCoh during successful stop trials for both younger and older adults, and for in- and anti-phase tACS (Supplementary Figure S12).

Before receiving anti-phase tACS, the response inhibition performance of younger adults was found to be significantly correlated with task-related rIFG-preSMA coupling during successful stop trials (Figure 6). However, this brain-behavior association was not significant in the pre-tACS task performance of the younger participants during their in-phase tACS sessions (Figure 6); this is indicative of an inconsistent relationship between task-related phase coupling and stop-signal task performance. The correlations between SSRTs and task-related ImCoh were not significant for the older participants before and after in- and anti-phase tACS (Supplementary Figure S13).

Figure 6

Cluster-Based Analyses of Correlation between SSRTs and ImCoh During Successful Stop Trials for Younger Participants

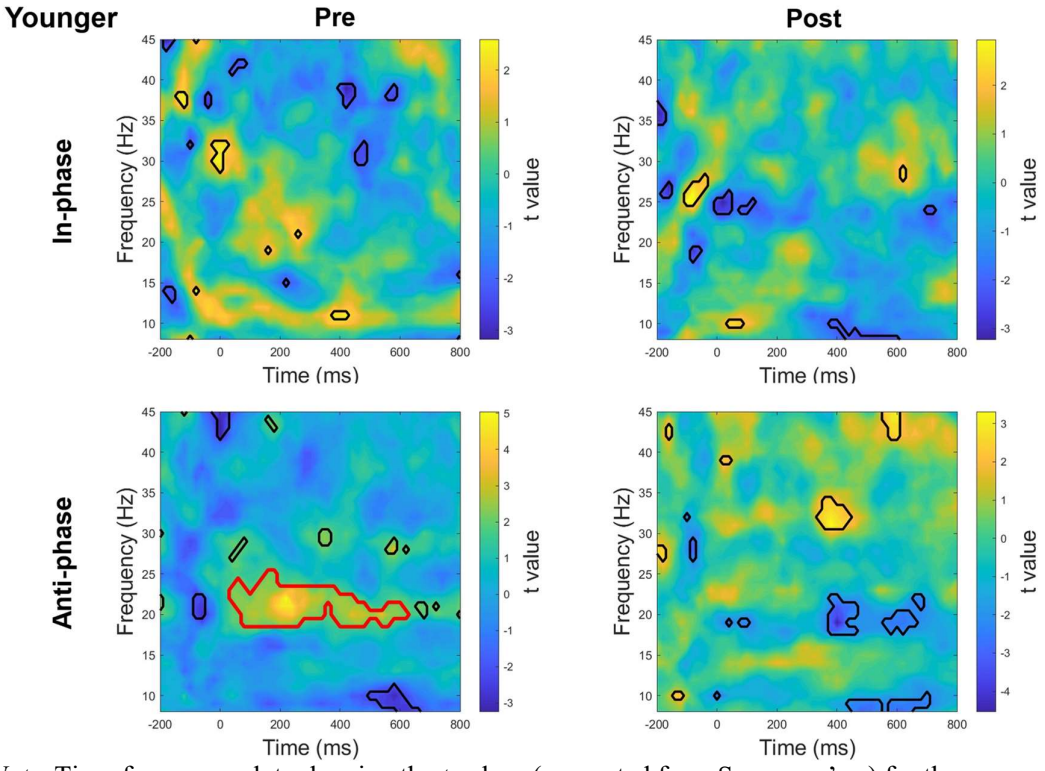

Note. Time-frequency plots showing the *t* values (converted from Spearman's ρ) for the correlation between ImCoh during successful stop trials and SSRT at each time-frequency point. Regions of suprathreshold clusters are denoted by black outlines ($p < 0.05$, uncorrected). A cluster in the anti-phase tACS condition at pre-tACS (outlined in red) was found to be significant after cluster-based correction. None of the clusters in the remaining conditions survived cluster-based correction.

The correlation between ΔImCoh and ΔSSRT was also assessed via cluster-based testing (Figure 7). A significant cluster was found for the older participants in the anti-phase tACS condition, with decreases in rIFG-preSMA phase-coupling during successful stop trials associated with increases in SSRTs – i.e., poorer response inhibition performance – for older adults during their anti-phase tACS sessions. The correlation between ΔImCoh and ΔSSRT was not significant for the older participants during their in-phase tACS sessions and for the younger participants in either in- or anti-phase tACS conditions (Figure 7).

Figure 7

Cluster-Based Analyses of Correlation between ΔSSRT and ΔImCoh for Older and Younger Participants

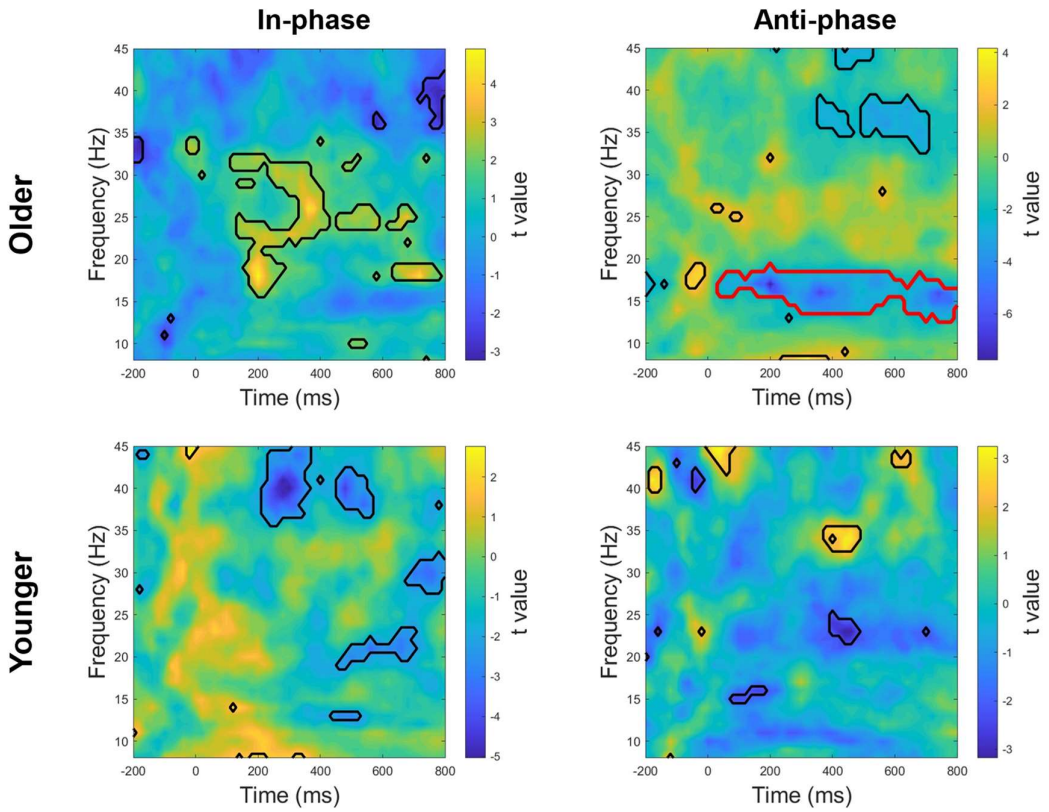

Note. Time-frequency plots showing the *t* values (converted from Spearman's ρ) for the correlation between ΔImCoh and ΔSSRT at each time-frequency point. Regions of suprathreshold clusters are denoted by black outlines ($p < 0.05$, uncorrected). A cluster in the anti-phase tACS condition at pre-tACS for the older participants (outlined in red) was found to be significant after cluster-based correction. None of the clusters in the remaining conditions survived cluster-based correction.

3.4.2. Follow-Up Analyses: tACS-Induced Changes in Spectral Power During Go Trials

The pre- to post-tACS changes in spectral power that occurred during *go* trials for the rIFG and preSMA were also analysed (see Supplementary Material for details). This was conducted as a follow-up analysis to explore the potential reasons for the longer go RTs exhibited by older participants after receiving in-phase tACS compared to pre stimulation (Section 3.2). The presence of beta activity on go trials has been linked to proactive inhibition (Jana et al., 2020) and increases in beta power from pre- to post-tACS would suggest that the slower responses of older participants after receiving in-phase tACS could be attributable to higher levels of proactive inhibition. This premise was supported by our findings: high beta and low gamma power ($\approx$ 22-35 Hz) in the rIFG during go trials were found to be significantly higher for older participants after in-phase tACS (Figure 8). Notably, these spectral changes occurred around 50 to 500 ms after imperative signal onset (Figure 8), which corresponded to the time window before the average go RT (529.31 ± 84.29 ms) for the older participants after receiving in-phase stimulation (Table 1). There were no other significant changes in spectral power from pre- to post-tACS for the older participants (Supplementary Figure S14). There were also no significant changes in spectral power at the rIFG and preSMA from either in- or anti-phase tACS for the younger participants (Supplementary Figure S14).

Figure 8

Results of Cluster-Based Analyses for Pre- to Post-tACS Changes in Spectral Power in rIFG during Go Trials

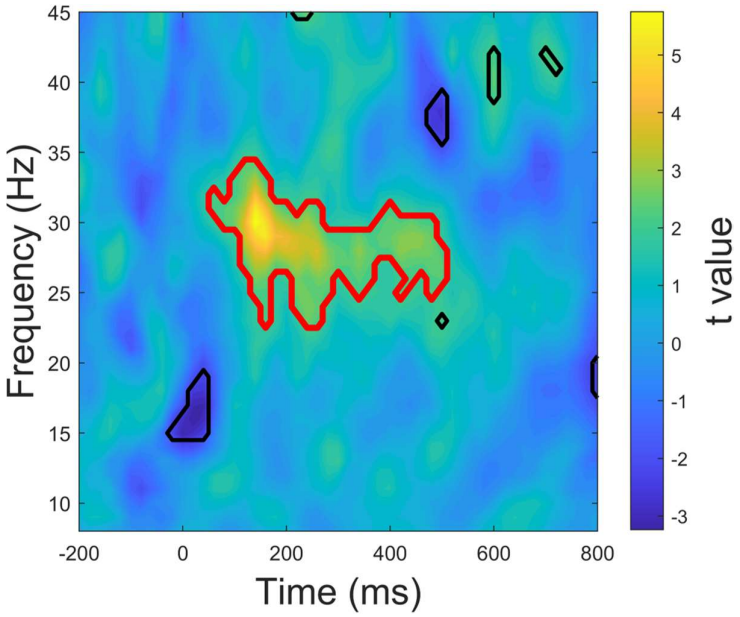

Note. Time-frequency plot showing the *t* values for all pre-tACS vs post-tACS contrasts. A cluster in the in-phase tACS condition for older participants (outlined in red) was found to be significant after cluster-based correction.

4. Discussion

4.1. In-phase tACS Improved SSRTs and Modulated Brain-Behavior Relationship in Younger but not Older Adults

Our primary hypothesis was that the delivery of in-phase tACS at the beta frequency of 20 Hz would strengthen the phase connectivity between the stimulated regions and lead to improvements in the efficiency of response inhibition (operationalized as SSRT) of healthy older and younger adults. Furthermore, on the basis that changes in functional connectivity potentially underlie cognitive declines in the healthy aging brain (which can impact executive control including response inhibition), we predicted that the performance gains from in-phase tACS would be more apparent in older participants. Conversely, anti-phase tACS was expected to weaken phase connectivity and degrade response inhibition.

Our hypotheses on the effects of in- and anti-phase beta tACS on response inhibition performance were partially supported, with younger participants exhibiting significant improvements in their response inhibition performance after receiving in-phase beta tACS. However, this performance boost from in-phase stimulation was not observed in the older adults, and neither age group exhibited statistically significant changes in response inhibition performance after receiving anti-phase tACS. The effects of stimulation on rIFG-preSMA connectivity assessed with EEG measures were also divergent from our initial hypotheses; specifically, post-tACS connectivity estimates for 8-45 Hz activity were not modulated by in- or anti-phase stimulation for both older and younger participants. The correlations between ΔImCoh and ΔSSRT also failed to reach statistical significance for both age groups and tACS conditions. However, stronger resting-state rIFG-preSMA phase-coupling in beta and gamma bands (17 to 41 Hz) was significantly associated with better response inhibition in younger participants after in-phase beta tACS. This suggests that in-phase beta tACS led to a significant brain-behavior correlation between response inhibition performance and rIFG-preSMA connectivity for the younger participants (Figure 5). The significant brain-behavior correlation for phase-coupling at beta- and gamma-band frequencies (17 to 41 Hz) also suggests that the post-tACS effects were the result of plasticity mechanisms rather than solely entrainment, since the latter would require after-effects to be confined to the beta-band (Vossen et al., 2015). Indeed, computational modelling and EEG connectivity analysis have found that connectivity changes after dual-site tACS could be accounted for by spike-timing dependent plasticity (Schwab et al., 2021).

However, the change in brain-behavior dynamics that resulted from in-phase tACS for younger participants was not accompanied by corresponding pre-post changes in ImCoh, nor in the association between ΔImCoh and ΔSSRT. We speculate that these outcomes were due to the disparity of tACS-induced field strengths in the stimulated regions. The electric field

simulations suggest that the field intensities induced by in- and anti-phase tACS were substantially weaker for the preSMA relative to rIFG (Figure 3). The disparity in field strengths between the two regions might have affected the entrainment and phase-locking of their neural activity during stimulation, which could affect the behavioral and electrophysiological outcomes of the tACS protocols. Hence, while in-phase tACS led to significant improvements in inhibitory performance and changes in brain-behavior relationship for the younger adults, the differential field intensities in the stimulated regions may have attenuated the effects of tACS such that pre-post changes in ImCoh were not significant.

The lack of pre-post changes in ImCoh could also have been partly a result of inter-individual variability in the tACS-induced effects on ImCoh from pre- to post-stimulation (Jamadar et al., 2010). The variability of the behavioral and neurophysiological outcomes of transcranial electrical stimulation has been well-documented (Antonenko et al., 2021; Guerra et al., 2020; Li et al., 2015). This was likewise observed by the wide confidence intervals in the pre-post changes in ImCoh after tACS (Supplementary Figure S1). Individual differences in the change in ImCoh might have inflated the error term in the pre-post contrast, such that group-level comparisons of ImCoh between the time points were not statistically significant. By contrast, the analysis of brain-behavior correlation at a specific time point allows the detection of any significant covariation that might exist between ImCoh and SSRTs (Jamadar et al., 2010). It was thus possible for the ImCoh-SSRT correlation to become significant despite the lack of pre-post changes in ImCoh at the group level, including the absence of a significant correlation between ΔImCoh and ΔSSRT.

One potential way of addressing the inter-individual variability in tACS effects might be through the individual optimisation of stimulation frequency (e.g., Reinhart & Nguyen, 2019). While this is certainly a possible solution, follow-up analyses of our study found

tACS-induced effects on SSRTs to be independent of the extent to which endogenous beta frequencies differed from the applied tACS frequency of 20 Hz (see Supplementary Material, Figures S15-18). This is congruent with previous research that found the modulation of resting-state alpha coherence by dual-site alpha tACS to be independent of individual alpha frequencies (Schwab et al., 2019). However, further empirical evidence is still required to ascertain the efficacy of an individualized protocol on response inhibition performance.

4.2. Age-Related Differences in tACS Outcomes

The lack of tACS-related effects in older individuals could be attributable to brain atrophy, which occurs as part of the normal aging process. This includes the loss of white and gray matter, with corresponding increases in cerebrospinal fluid volume (CSF) (Courchesne et al., 2000; Lemaître et al., 2005). Higher levels of atrophy have been associated with smaller amounts of tACS currents reaching cortical regions – resulting in currents being 'shunted' away by CSF because of its superior conductivity over brain tissue (Indahlastari et al., 2020). It is thus possible that the lack of significant changes in inhibitory performance in the older individuals was due to insufficient tACS currents reaching rIFG and preSMA. Similarly, the heterogeneity of tACS outcomes in both younger and older individuals could be the result of inter-individual differences in brain anatomy, which contributes to the variability of peak field magnitude or spatial distribution of tACS-induced electric fields across individuals (Antonenko et al., 2021; Kasten et al., 2019). A potential way of mitigating this variability is the use of subject-specific tACS intensities, by using electric field simulations based on individual brain anatomy to determine the current intensities that would achieve the desired electric field densities at target regions (Indahlastari et al., 2020). Admittedly, this approach could be costly and time-consuming, as MRI scans would be required to obtain each individual's anatomical data.

4.3. tACS-Related Changes in go RTs

In addition to inhibitory performance, we also analysed the effects of tACS on response speeds in go trials (go RTs). We found that in-phase tACS had opposite effects on the go RTs of younger and older participants: whereas the younger participants had faster responses on go trials after stimulation, the older adults exhibited longer reaction times at post-tACS.

Previous research has found that the rapid generation of planned movements and shorter reaction times are facilitated by pre-movement suppression of specific inputs from the motor cortex to the corticospinal system (Duque & Ivry, 2009; Fujiyama et al., 2011; Hannah et al., 2018), which corroborates the dynamical systems view that the coexistence of excitation and inhibition is vital to successful movement preparation (Kaufman et al., 2014, 2016). It is possible that the delivery of in-phase tACS over preSMA and rIFG resulted in down-stream suppression of specific activity in the motor cortex, through the fronto-basal-ganglia network (Tan et al., 2019), thus boosting movement generation and reducing reaction time of the younger participants. However, this can only be verified via further investigation involving the assessment of corticospinal activity and is beyond the scope of the current study. Furthermore, it remains unclear as to why the go RTs of older participants were not similarly reduced by in-phase tACS. Instead, their go RTs were increased after in-phase stimulation, which is indicative of an overall slowing in motor activity. This might be due to an increase in proactive inhibition, whereby individuals engage in preparatory behaviors that facilitate motor inhibition (Liebrand et al., 2017). Indeed, our analyses of the pre- to post-tACS changes in spectral power during go trials found that beta power at the rIFG was significantly increased by in-phase tACS for the older participants (Figure 8). Notably, the significant increase in power began shortly after the onset of the imperative signal and subsided approximately before the average go RT of the older individuals. This finding is in

accordance with a possible increase in proactive inhibition during anticipation of a possible stop-signal onset, beginning soon after the imperative signal was presented and terminating upon the execution of the go response (Jana et al., 2020). Consequently, the go responses of the older participants might have been delayed by their higher levels of proactive inhibition (Lavallee et al., 2014).

We wish to note that the stop-signal task in the current study was not designed to measure proactive inhibition. This typically requires the comparison between cued and uncued stop trials, where the cues provide information about imminent stop signals and thus influence proactive control – i.e., the anticipatory and preparatory behaviors taken by individuals to improve subsequent inhibitory performance (e.g., Lavallee et al., 2014; Smittenaar et al., 2015). As such, we could not verify that proactive inhibition was truly increased in the older adults after in-phase tACS and was thus responsible for their longer reaction times. Moreover, the reasons behind the differential effects of in-phase stimulation on the go RTs of the younger participants remained elusive: their go RTs were actually shorter after in-phase tACS. There were also no significant spectral power changes in the younger participants that were indicative of changes in proactive inhibition. Further research is thus required to elucidate these age-related differences in the effects of in-phase tACS on response times.

4.4. Task-Related ImCoh and Stop-Signal Performance

Our analyses of task-related rIFG-preSMA ImCoh (i.e., during successful stop trials) revealed that it was not significantly modulated by either in- or anti-phase tACS in both younger and older participants. Additionally, there were no significant associations between the SSRTs and task-related rIFG-preSMA ImCoh for the older participants before and after receiving in- and anti-phase tACS.

Similarly, SSRTs were not significantly correlated with task-related rIFG-preSMA connectivity for the younger adults after receiving in- or anti-phase tACS. At the same time, we found that longer SSRTs (poorer response inhibition) were associated with stronger task-related beta-band phase-coupling for the younger participants before receiving anti-phase tACS, but not before in-phase tACS. This inter-session difference in pre-tACS brain-behavior relationship suggests that response inhibition performance might not be subserved by task-related phase-coupling between the rIFG and preSMA.

Our analyses also revealed a significant relationship between the pre- to post-tACS changes in SSRTs and rIFG-preSMA phase-coupling in successful stop trials (ΔSSRT and ΔImCoh) for the older participants, such that declines or smaller improvements in inhibitory performance were associated with decreases or smaller increases in connectivity at low beta frequencies after anti-phase tACS. Analogously, increases or smaller decreases in rIFG-preSMA beta coupling in successful stop trials were related to improvements or smaller declines in response inhibition for the older participants when anti-phase tACS was applied. Considering that there were no corresponding changes in the SSRTs of older individuals, this relationship between ΔSSRT and ΔImCoh does not appear to be practically meaningful, despite it being statistically significant. Similarly, the association between ΔSSRT and ΔImCoh was not statistically significant for the younger participants in either of their in- or anti-phase tACS sessions – this is incongruent with the improvement of inhibitory performance that only occurred after in-phase tACS. Again, our findings suggest that *task-related* phase-coupling between the rIFG and preSMA might not underlie response inhibition performance.

4.5. Limitations

A key limitation was the disparity in tACS-induced field strengths at the rIFG and preSMA (see more details in 4.1). Another limitation of the current study was that EEG could not be recorded during tACS, and we were thus unable to explore peri-tACS electrophysiological activity. Due to the nature of the EEG caps that were used, whereby a net system of electrode sensors is connected by stretchy elastic bands, tACS electrodes could not be placed on the head without shifting the EEG sensors and affecting their contact with the scalp. Without online measurements of electrophysiological activity, we could not verify the occurrence of peri-stimulation entrainment. Despite the absence of online EEG data, we wish to note that the entrainment of neural activity during tACS has been demonstrated in previous research (Helfrich, Schneider, et al., 2014). Finally, the lack of a sham condition also prevents a more conclusive investigation of the effects of in- and anti-phase stimulation on response inhibition and rIFG-preSMA connectivity.

5. Conclusions

The main objective of this paper was two-fold. Firstly, to investigate the efficacy of dual-site tACS over the rIFG and preSMA in ameliorating age-related declines in response inhibition. Secondly, to gain further insight into the neural underpinnings of response inhibition in healthy older individuals. It was posited that the application of in-phase rIFG-preSMA tACS at the beta frequency of 20 Hz would improve response inhibition for both healthy younger and healthy older individuals. This hypothesis was partially supported by our findings, with in-phase stimulation significantly improving the response inhibition performance of the younger participants, but not their older counterparts. The younger participants' improvement in response inhibition could potentially be attributable to the strengthening of the brain-behavior relationship between their inhibitory performance and

rIFG-preSMA phase-coupling after in-phase tACS. Conversely, the lack of significant behavioral improvements for the older participants might stem from individual variability in age-related changes in brain anatomy. Age-related atrophy in brain matter could have also attenuated the amount of tACS current flow that was received by the rIFG and preSMA in the older participants.

To conclude, while rIFG-preSMA beta tACS appears to be efficacious in facilitating inhibitory performance of healthy younger adults, its effects in healthy older individuals were subject to considerable heterogeneity. Despite the lack of clear evidence supporting the efficacy of this tACS protocol in alleviating age-related declines in response inhibition, we believe that the findings of this paper have provided important insights into the neural underpinnings of inhibitory performance and contributed to a broader mechanistic understanding of the effects of dual-site tACS on functional connectivity.

Acknowledgements

Funding

This work was supported by the Australia-Germany Joint Research Co-operation (DAAD) (57384703) awarded to H.F, M.A.N, and J.T, the Dementia Australia Research Foundation (711-1641) awarded to HF, MAN, and MRH. MRH was supported by the Australian Research Council Discovery Scheme (FT150100406; DP200101696).

Declaration of Competing Interests

The authors declare no competing interests.

References

Antal, A., & Herrmann, C. S. (2016). Transcranial alternating current and random noise stimulation: Possible mechanisms. *Neural Plasticity*, *2016*, 12. https://doi.org/10.1155/2016/3616807

Antonenko, D., Grittner, U., Saturnino, G., Nierhaus, T., Thielscher, A., & Flöel, A. (2021). Inter-individual and age-dependent variability in simulated electric fields induced by conventional transcranial electrical stimulation. *NeuroImage*, *224*, 117413. https://doi.org/10.1016/j.neuroimage.2020.117413

Aron, A. R., Herz, D. M., Brown, P., Forstmann, B. U., & Zaghloul, K. (2016). Frontosubthalamic circuits for control of action and cognition. *The Journal of Neuroscience*, *36*(45), 11489. https://doi.org/10.1523/JNEUROSCI.2348-16.2016

Band, G. P. H., van der Molen, M. W., & Logan, G. D. (2003). Horse-race model simulations of the stop-signal procedure. *Acta Psychologica*, *112*(2), 105–142. https://doi.org/10.1016/S0001-6918(02)00079-3

Brown, C. A., Schmitt, F. A., Smith, C. D., & Gold, B. T. (2019). Distinct patterns of default mode and executive control network circuitry contribute to present and future executive function in older adults. *NeuroImage*, *195*, 320–332. https://doi.org/10.1016/j.neuroimage.2019.03.073

Carson, N., Leach, L., & Murphy, K. J. (2018). A re-examination of Montreal Cognitive Assessment (MoCA) cutoff scores. *International Journal of Geriatric Psychiatry*, *33*(2), 379–388. https://doi.org/10.1002/gps.4756

Chatrian, G. E., Lettich, E., & Nelson, P. L. (1985). Ten Percent Electrode System for Topographic Studies of Spontaneous and Evoked EEG Activities. *American Journal of EEG Technology*, *25*(2), 83–92. https://doi.org/10.1080/00029238.1985.11080163

Chong, J. S. X., Ng, K. K., Tandi, J., Wang, C., Poh, J.-H., Lo, J. C., Chee, M. W. L., & Zhou, J. H. (2019). Longitudinal changes in the cerebral cortex functional organization of healthy elderly. *The Journal of Neuroscience*, *39*(28), 5534. https://doi.org/10.1523/JNEUROSCI.1451-18.2019

Cohen, M. X. (2014). *Analyzing Neural Time Series Data*. The MIT Press. https://mitpress.mit.edu/books/analyzing-neural-time-series-data

Courchesne, E., Chisum, H. J., Townsend, J., Cowles, A., Covington, J., Egaas, B., Harwood, M., Hinds, S., & Press, G. A. (2000). Normal Brain Development and Aging: Quantitative Analysis at in Vivo MR Imaging in Healthy Volunteers. *Radiology*, *216*(3), 672–682. https://doi.org/10.1148/radiology.216.3.r00au37672

Duque, J., & Ivry, R. B. (2009). Role of corticospinal suppression during motor preparation. *Cerebral Cortex (New York, N.Y.: 1991)*, *19*(9), 2013–2024. https://doi.org/10.1093/cercor/bhn230

Fertonani, A., Ferrari, C., & Miniussi, C. (2015). What do you feel if I apply transcranial electric stimulation? Safety, sensations and secondary induced effects. *Clinical Neurophysiology*, *126*(11), 2181–2188. https://doi.org/10.1016/j.clinph.2015.03.015

Firke, S. (2021). *janitor: Simple Tools for Examining and Cleaning Dirty Data*. https://github.com/sfirke/janitor

Fox, J., & Friendly, M. (2021). *heplots: Visualizing Hypothesis Tests in Multivariate Linear Models*. http://friendly.github.io/heplots/

Fox, J., Weisberg, S., & Price, B. (2020). *car: Companion to Applied Regression*. https://CRAN.R-project.org/package=car

Fries, P. (2005). A mechanism for cognitive dynamics: Neuronal communication through neuronal coherence. *Trends in Cognitive Sciences*, *9*(10), 474–480. https://doi.org/10.1016/j.tics.2005.08.011

Fries, P. (2015). Rhythms for cognition: Communication through coherence. *Neuron*, *88*(1), 220–235. ProQuest Central. https://doi.org/10.1016/j.neuron.2015.09.034

Fujiyama, H., Tandonnet, C., & Summers, J. J. (2011). Age-related differences in corticospinal excitability during a Go/NoGo task. *Psychophysiology*, *48*(10), 1448–1455. https://doi.org/10.1111/j.1469-8986.2011.01201.x

Guerra, A., López-Alonso, V., Cheeran, B., & Suppa, A. (2020). Solutions for managing variability in non-invasive brain stimulation studies. *Neuroscience Letters*, *719*, 133332. https://doi.org/10.1016/j.neulet.2017.12.060

Hannah, R., Cavanagh, S. E., Tremblay, S., Simeoni, S., & Rothwell, J. C. (2018). Selective suppression of local interneuron circuits in human motor cortex contributes to movement preparation. *The Journal of Neuroscience*, *38*(5), 1264–1276. PMC. https://doi.org/10.1523/JNEUROSCI.2869-17.2017

Harrell, F. E., Jr. (2021). *Hmisc: Harrell Miscellaneous*. https://CRAN.R-project.org/package=Hmisc

Helfrich, R. F., Knepper, H., Nolte, G., Strüber, D., Rach, S., Herrmann, C. S., Schneider, T. R., & Engel, A. K. (2014). Selective modulation of interhemispheric functional connectivity by HD-tACS shapes perception. *PLOS Biology*, *12*(12), 1–15. https://doi.org/10.1371/journal.pbio.1002031

Helfrich, R. F., Schneider, T. R., Rach, S., Trautmann-Lengsfeld, S. A., Engel, A. K., & Herrmann, C. S. (2014). Entrainment of brain oscillations by transcranial alternating current stimulation. *Current Biology*, *24*(3), 333–339. https://doi.org/10.1016/j.cub.2013.12.041

Hermans, L., Leunissen, I., Pauwels, L., Cuypers, K., Peeters, R., Puts, N. A. J., Edden, R. A. E., & Swinnen, S. P. (2018). Brain GABA levels are associated with inhibitory

control deficits in older adults. *The Journal of Neuroscience*, *38*(36), 7844–7851. https://doi.org/10.1523/JNEUROSCI.0760-18.2018

Hogeveen, J., Grafman, J., Aboseria, M., David, A., Bikson, M., & Hauner, K. K. (2016). Effects of high-definition and conventional tDCS on response inhibition. *Brain Stimulation*, *9*(5), 720–729. https://doi.org/10.1016/j.brs.2016.04.015

Hsu, T.-Y., Tseng, L.-Y., Yu, J.-X., Kuo, W.-J., Hung, D. L., Tzeng, O. J. L., Walsh, V., Muggleton, N. G., & Juan, C.-H. (2011). Modulating inhibitory control with direct current stimulation of the superior medial frontal cortex. *NeuroImage*, *56*(4), 2249–2257. https://doi.org/10.1016/j.neuroimage.2011.03.059

Indahlastari, A., Albizu, A., O'Shea, A., Forbes, M. A., Nissim, N. R., Kraft, J. N., Evangelista, N. D., Hausman, H. K., & Woods, A. J. (2020). Modeling transcranial electrical stimulation in the aging brain. *Brain Stimulation: Basic, Translational, and Clinical Research in Neuromodulation*, *13*(3), 664–674. https://doi.org/10.1016/j.brs.2020.02.007

Jacobson, L., Javitt, D. C., & Lavidor, M. (2011). Activation of inhibition: Diminishing impulsive behavior by direct current stimulation over the inferior frontal gyrus. *Journal of Cognitive Neuroscience*, *23*(11), 3380–3387. https://doi.org/10.1162/jocn_a_00020

Jamadar, S., Hughes, M., Fulham, W. R., Michie, P. T., & Karayanidis, F. (2010). The spatial and temporal dynamics of anticipatory preparation and response inhibition in task-switching. *NeuroImage*, *51*(1), 432–449. https://doi.org/10.1016/j.neuroimage.2010.01.090

Jana, S., Hannah, R., Muralidharan, V., & Aron, A. R. (2020). Temporal cascade of frontal, motor and muscle processes underlying human action-stopping. *ELife*, *9*, e50371. https://doi.org/10.7554/eLife.50371

Kassambara, A. (2020). *ggpubr: Ggplot2 Based Publication Ready Plots*. https://rpkgs.datanovia.com/ggpubr/

Kassambara, A. (2021). *rstatix: Pipe-Friendly Framework for Basic Statistical Tests*. https://rpkgs.datanovia.com/rstatix/

Kasten, F. H., Duecker, K., Maack, M. C., Meiser, A., & Herrmann, C. S. (2019). Integrating electric field modeling and neuroimaging to explain inter-individual variability of tACS effects. *Nature Communications*, *10*(1), 5427. https://doi.org/10.1038/s41467-019-13417-6

Kaufman, M. T., Churchland, M. M., Ryu, S. I., & Shenoy, K. V. (2014). Cortical activity in the null space: Permitting preparation without movement. *Nature Neuroscience*, *17*(3), Article 3. https://doi.org/10.1038/nn.3643

Kaufman, M. T., Seely, J. S., Sussillo, D., Ryu, S. I., Shenoy, K. V., & Churchland, M. M. (2016). The Largest Response Component in the Motor Cortex Reflects Movement Timing but Not Movement Type. *ENeuro*, *3*(4). https://doi.org/10.1523/ENEURO.0085-16.2016

Krause, M. R., Vieira, P. G., Csorba, B. A., Pilly, P. K., & Pack, C. C. (2019). Transcranial alternating current stimulation entrains single-neuron activity in the primate brain. *Proceedings of the National Academy of Sciences*, 1–9. https://doi.org/10.1073/pnas.1815958116

Lavallee, C. F., Meemken, M. T., Herrmann, C. S., & Huster, R. J. (2014). When holding your horses meets the deer in the headlights: Time-frequency characteristics of global and selective stopping under conditions of proactive and reactive control. *Frontiers in Human Neuroscience*, *8*(994). https://doi.org/10.3389/fnhum.2014.00994

Lemaître, H., Crivello, F., Grassiot, B., Alpérovitch, A., Tzourio, C., & Mazoyer, B. (2005). Age- and sex-related effects on the neuroanatomy of healthy elderly. *NeuroImage*,

26(3), 900–911. http://dx.doi.org.libproxy.murdoch.edu.au/10.1016/j.neuroimage.2005.02.042

Li, L. M., Uehara, K., & Hanakawa, T. (2015). The contribution of interindividual factors to variability of response in transcranial direct current stimulation studies. *Frontiers in Cellular Neuroscience*, *9*, 1–19. https://doi.org/10.3389/fncel.2015.00181

Liebrand, M., Pein, I., Tzvi, E., & Krämer, U. M. (2017). Temporal dynamics of proactive and reactive motor inhibition. *Frontiers in Human Neuroscience*, *11*, 1–14. https://doi.org/10.3389/fnhum.2017.00204

Logan, G. D., & Cowan, W. B. (1984). On the ability to inhibit thought and action: A theory of an act of control. *Psychological Review*, *91*(3), 295–327. PsycARTICLES. https://doi.org/10.1037/0033-295X.91.3.295

Mangiafico, S. (2021). *rcompanion: Functions to Support Extension Education Program Evaluation*. http://rcompanion.org/

Maris, E. (2012). Statistical testing in electrophysiological studies. *Psychophysiology*, *49*(4), 549–565. https://doi.org/10.1111/j.1469-8986.2011.01320.x

Maris, E., Schoffelen, J.-M., & Fries, P. (2007). Nonparametric statistical testing of coherence differences. *Journal of Neuroscience Methods*, *163*(1), 161–175. https://doi.org/10.1016/j.jneumeth.2007.02.011

Miyake, A., Friedman, N. P., Emerson, M. J., Witzki, A. H., Howerter, A., & Wager, T. D. (2000). The unity and diversity of executive functions and their contributions to complex “frontal lobe” tasks: A latent variable analysis. *Cognitive Psychology*, *41*(1), 49–100. https://doi.org/10.1006/cogp.1999.0734

Nasreddine, Z. S., Rossetti, H., Phillips, N., Chertkow, H., Lacritz, L., Cullum, M., & Weiner, M. (2012). Normative data for the Montreal Cognitive Assessment (MoCA)

in a population-based sample: Author response. *Neurology*, *78*(10), 765–766. https://doi.org/10.1212/01.wnl.0000413072.54070.a3

Neuwirth, E. (2014). *RColorBrewer: ColorBrewer Palettes*. https://CRAN.R-project.org/package=RColorBrewer

Nolte, G., Bai, O., Wheaton, L., Mari, Z., Vorbach, S., & Hallett, M. (2004). Identifying true brain interaction from EEG data using the imaginary part of coherency. *Clinical Neurophysiology*, *115*(10), 2292–2307. https://doi.org/10.1016/j.clinph.2004.04.029

Oldfield, R. C. (1971). The assessment and analysis of handedness: The Edinburgh inventory. *Neuropsychologia*, *9*(1), 97–113. https://doi.org/10.1016/0028-3932(71)90067-4

Peeters, M. J. (2016). Practical significance: Moving beyond statistical significance. *Currents in Pharmacy Teaching and Learning*, *8*(1), 83–89. https://doi.org/10.1016/j.cptl.2015.09.001

Peirce, J., Gray, J. R., Simpson, S., MacAskill, M., Höchenberger, R., Sogo, H., Kastman, E., & Lindeløv, J. K. (2019). PsychoPy2: Experiments in behavior made easy. *Behavior Research Methods*, *51*(1), 195–203. https://doi.org/10.3758/s13428-018-01193-y

Polanía, R., Nitsche, M. A., Korman, C., Batsikadze, G., & Paulus, W. (2012). The importance of timing in segregated theta phase-coupling for cognitive performance. *Current Biology*, *22*(14), 1314–1318. https://doi.org/10.1016/j.cub.2012.05.021

R Core Team. (2019). *R: A language and environment for statistical computing. R Foundation for Statistical Computing*. https://www.R-project.org/

Reinhart, R. M. G., & Nguyen, J. A. (2019). Working memory revived in older adults by synchronizing rhythmic brain circuits. *Nature Neuroscience*, *22*(5), 820–827. https://doi.org/10.1038/s41593-019-0371-x

Rudis, B. (2020). *hrbrthemes: Additional Themes, Theme Components and Utilities for ggplot2*. http://github.com/hrbrmstr/hrbrthemes

Salinas, E., & Sejnowski, T. J. (2001). Correlated neuronal activity and the flow of neural information. *Nature Reviews. Neuroscience*, *2*(8), 539–550. ProQuest Central. https://doi.org/10.1038/35086012

Schoene, D., Delbaere, K., & Lord, S. R. (2017). Impaired response selection during stepping predicts falls in older people—A cohort study. *Journal of the American Medical Directors Association*, *18*(8), 719–725. https://doi.org/10.1016/j.jamda.2017.03.010

Schwab, B. C., König, P., & Engel, A. K. (2021). Spike-timing-dependent plasticity can account for connectivity aftereffects of dual-site transcranial alternating current stimulation. *NeuroImage*, *237*, 118179. https://doi.org/10.1016/j.neuroimage.2021.118179

Schwab, B. C., Misselhorn, J., & Engel, A. K. (2019). Modulation of large-scale cortical coupling by transcranial alternating current stimulation. *Brain Stimulation: Basic, Translational, and Clinical Research in Neuromodulation*. https://doi.org/10.1016/j.brs.2019.04.013

Siegel, M., Donner, T. H., & Engel, A. K. (2012). Spectral fingerprints of large-scale neuronal interactions. *Nature Reviews. Neuroscience*, *13*(2), 121–134. ProQuest Central. https://doi.org/10.1038/nrn3137

Signorell, A. (2021). *DescTools: Tools for Descriptive Statistics*. https://CRAN.R-project.org/package=DescTools

Smittenaar, P., Rutledge, R. B., Zeidman, P., Adams, R. A., Brown, H., Lewis, G., & Dolan, R. J. (2015). Proactive and reactive response inhibition across the lifespan. *PLoS ONE*, *10*(10). Scopus. https://doi.org/10.1371/journal.pone.0140383

Swann, N. C., Poizner, H., Houser, M., Gould, S., Greenhouse, I., Cai, W., Strunk, J., George, J., & Aron, A. R. (2011). Deep brain stimulation of the subthalamic nucleus alters the cortical profile of response inhibition in the beta frequency band: A scalp

EEG study in Parkinson's disease. *The Journal of Neuroscience*, *31*(15), 5721. https://doi.org/10.1523/JNEUROSCI.6135-10.2011

Tan, J., Iyer, K. K., Tang, A. D., Jamil, A., Martins, R. N., Sohrabi, H. R., Nitsche, M. A., Hinder, M. R., & Fujiyama, H. (2019). Modulating functional connectivity with non-invasive brain stimulation for the investigation and alleviation of age-associated declines in response inhibition: A narrative review. *NeuroImage*, *185*, 490–512. https://doi.org/10.1016/j.neuroimage.2018.10.044

Tsvetanov, K. A., Ye, Z., Hughes, L., Samu, D., Treder, M. S., Wolpe, N., Tyler, L. K., & Rowe, J. B. (2018). Activity and connectivity differences underlying inhibitory control across the adult lifespan. *The Journal of Neuroscience*, *38*(36), 7887–7900. https://doi.org/10.1523/jneurosci.2919-17.2018

Verbruggen, F., Aron, A. R., Band, G. P. H., Beste, C., Bissett, P. G., Brockett, A. T., Brown, J. W., Chamberlain, S. R., Chambers, C. D., Colonius, H., Colzato, L. S., Corneil, B. D., Coxon, J. P., Dupuis, A., Eagle, D. M., Garavan, H., Greenhouse, I., Heathcote, A., Huster, R. J., … Boehler, C. N. (2019). A consensus guide to capturing the ability to inhibit actions and impulsive behaviors in the stop-signal task. *ELife*, *8*, e46323. https://doi.org/10.7554/eLife.46323

Vossen, A., Gross, J., & Thut, G. (2015). Alpha power increase after transcranial alternating current stimulation at alpha frequency (α-tACS) reflects plastic changes rather than entrainment. *Brain Stimulation*, *8*(3), 499–508. https://doi.org/10.1016/j.brs.2014.12.004

Wickham, H. (2020). *Reshape2: Flexibly Reshape Data: A Reboot of the Reshape Package*. https://github.com/hadley/reshape

Wickham, H. (2021). *tidyverse: Easily Install and Load the Tidyverse*. https://CRAN.R-project.org/package=tidyverse

Wischnewski, M., Engelhardt, M., Salehinejad, M. A., Schutter, D. J. L. G., Kuo, M. F., & Nitsche, M. A. (2018). NMDA receptor-mediated motor cortex plasticity after 20 Hz transcranial alternating current stimulation. *Cerebral Cortex*, bhy160–bhy160. https://doi.org/10.1093/cercor/bhy160

Womelsdorf, T., Schoffelen, J.-M., Oostenveld, R., Singer, W., Desimone, R., Engel, A. K., & Fries, P. (2007). Modulation of neuronal interactions through neuronal synchronization. *Science*, *316*(5831), 1609–1612. https://doi.org/10.1126/science.ll39178

Xu, B., Sandrini, M., Wang, W.-T., Smith, J. F., Sarlls, J. E., Awosika, O., Butman, J. A., Horwitz, B., & Cohen, L. G. (2016). PreSMA stimulation changes task-free functional connectivity in the fronto-basal-ganglia that correlates with response inhibition efficiency. *Human Brain Mapping*, *37*(9), 3236–3249. https://doi.org/10.1002/hbm.23236